Tanzania Journal of Science 47(1): 228-242, 2021
ISSN 0856-1761, e-ISSN 2507-7961


# Multi-Bands Circular Ring Monopole Antenna with Double L-Shape for WLAN/WiMAX Applications

**Hassan Y Mkindu[1] and Hashim U Iddi[2]**

*[1]Department of Electrical Engineering, College of Engineering and Technologies, University of Dar es Salaam, P. O. Box 35131, Dar es Salaam, Tanzania*

*[2]Department of Electronics and Telecommunication Engineering, College of Information and Communication Technologies, University of Dar es Salaam, P. O. Box 33335, Dar es Salaam, Tanzania*

*Corresponding author, e-mail: hashimuledi@udsm.ac.tz; hashimuledi@gmail.com*

*Co-author's e-mail: hmkindu@gmail.com*

Received 29 Sep 2020, Revised 10 Dec 2020, Accepted 28 Dec 2020, Published Feb 2021

https://dx.doi.org/10.4314/tjs.v47i1.20

**Abstract**

The rapid growth of technology increases the demands of low profile and compact antennas, supporting different wireless systems standards in mobile devices. Recently, several multi-band antenna designs have been proposed for mobile devices due to the current advancement of antenna technology. In this paper, a multi-band circular ring with a double L-shaped monopole antenna for Wireless Local Area Network (WLAN) and Worldwide Interoperability for Microwave Access (WiMAX) applications is presented. The proposed antenna consists of a circular-shaped and rectangular strip connected with two inverted L-shaped trips. The H-shaped-strips are attached within the rectangular-strips. The antenna is fed by a 50 Ω micro-strip line, and it operates at three resonant frequencies, which include 2.4 GHz and 3.5/5.5 GHz for WLAN and WiMAX applications, respectively. The antenna has been simulated using CST Microwave Studio software. The proposed antenna achieved impedance bandwidth of 284 MHz, 368 MHz, and 1120 MHz for 2.4 GHz, 3.5 GHz, and 5.5 GHz frequency bands, respectively, while the corresponding antenna gains are 1.28 dB, 1.78 dB, and 2.78 dB. The antenna has a compact dimension size of 18 x 28 x 1.6 $mm^3$ when printed on the FR-4 substrate of dielectric constant 4.3.

**Keywords**: monopole antenna, multi-band antenna, WLAN, WiMAX and inverted L-shaped strips.

## Introduction

The fast growth in wireless communications has increased the demands for developing antennas supporting different wireless systems standards in mobile devices. Due to space constraints in mobile devices, there is a need to design an antenna structure that can cover multiple frequency bands rather than employing several antennas for each wireless standard with a low profile and compact structure (Pal et al. 2020). The use of several antennas for each frequency band leads to large space requirements in mobile devices. Various wireless technology systems such as GSM (900/1800 MHz), WCDMA/UMTS (1885/2025 MHz), Bluetooth (2.4 GHz), WLAN (2.4/5.2/5.8 GHz), WiMAX (2.5/3.5/5.5 GHz), and GPS (1575.42/1227.60 MHz) have been highly integrated into the mobile devices. To fulfil the RF system requirements using the different frequency bands, antenna technology that can provide wideband characteristics is required.

Various microstrip antenna (MSA) designs are widely used due to their attractive features such as low profile, conformal, lightweight, and least manufacturing costs (Raju 2009). Due to this, MSAs are well suited for WLAN and WiMAX application systems (Yao et al. 2020). However, the original microstrip antenna or antenna array's electrical performance suffers from some serious drawbacks, including very narrow bandwidth, high feed network losses, high cross-polarization, and low power handling capacity (Fang 2009). Previous researchers proposed several techniques to improve bandwidth, return loss, and radiation characteristics. The printed monopole antennas have been widely studied for various wireless communications using different geometric structures. These include antennas such as a paw-shaped multi-band monopole antenna for WLAN and WiMAX applications, which used three arms to achieve multi-band frequency (Song et al. 2011). The use of a trapezoidal ground in Thomas and Sreenivasan (2009) and circular slot with triangular truncations in Mallik et al. (2012) have been used to achieve the narrow triple-band frequencies. According to Liu and Hsu (2005), a flared shape with V-sleeve or Y-shape to realize the multi-band operation was reported. S-shaped meander strip and a C-shaped strip investigated in Li et al. (2010). A circular ring, a Y-shaped- strip, with a defected ground plane was discussed in Pei et al. (2011). Additionally, recent multi-band antenna researches have been presented (Weng et al. 2008, Zhang et al. 2012, Wang et al. 2012, Li et al. 2012, El Misilmani et al. 2012, Huang et al. 2014, Ellis et. 2014, Gautam et al. 2015, Liu et al. 2017, Sang et al. 2017, Chouti et al. 2017, Ali et al. 2018, Kumar et al. 2018, Pandit and Harish 2018, Patel and Upadhyaya 2019, Saraswat and Kumar 2020) covering WLAN and WiMAX bands, which used techniques such as slotting, defective ground structure, and use of parasitic elements. However, the complex structures, large antenna size, narrow bandwidth of these antennas, which cannot cover full the required bands, make them difficult to be implemented in small devices for WLAN/WiMAX applications (Chetal et al. 2019).

This paper presents a multi-band circular ring with a double L-shaped monopole antenna for WLAN and WiMAX applications. The proposed antenna consists of a circular-shaped and rectangular strip connected with two inverted L- shaped trips. H-shaped-strips are attached within the rectangular-strips. A 50 Ω micro-strip line feeds the antenna, and it operates at three resonant frequencies, including 2.4 GHz and 3.5/5.5 GHz for WLAN and WiMAX applications, respectively. The antenna has been simulated using CST Microwave Studio software and obtained wide multi-band coverage with high antenna gains and small-size antenna structure compared to the recently proposed antenna design.

## Materials and Methods

### Antenna design process

The proposed antenna was designed and simulated using CST Microwave studio. The antenna consists of a circular-shaped strip connected with a rectangular-strip to form the top part. Two inverted L-shaped trips are attached at the rectangular strip ends, and H-shaped-strips are attached within the rectangular-strips. The antenna was designed on a 1.6 mm thick FR-4 substrate with a relative permittivity of 4.3. A 50 Ω micro-strip line is attached to a circular patch with a signal width of 3 mm used as feed to the antenna. The proposed multi-band antenna design processes are shown in Figure 1 (a)–(d). The design of the first geometry of the proposed antenna is obtained by considering the circular patch with the radius ($r$) as in Equation (1) (Gupta 2009, Aghda et al. 2012).

$$r = \frac{87.91}{f_r\sqrt{\epsilon_r}} \qquad (1)$$

Where: $f_r$ is the resonant frequency in GHz, and $\epsilon_r$ represents the dielectric constant of the substrate in Coulombs squared per Newton-square meter. The first estimated value of the circular patch radius was calculated by substituting the value of the first resonant frequency (2.4 GHz) and the dielectric constant of the substrate.

The antenna design 1 shown in Figure 1 (a) provides two resonant frequencies at 3.59 GHz and 5.4 GHz with the return loss values of -22.28 dB and -26.96 dB, respectively. The two resonant frequencies were created by the introduction of a circular ring structure. In antenna design 2 shown in Figure 1 (b), a rectangular ring was introduced, and the effects of shifting of 3.59 GHz resonant frequency to a lower frequency band was observed. The third geometry of antenna 3, two L-shaped structures were added, which resulted in three resonant frequencies, which are 2.67 GHz, 3.56 GHz, and 5.25 GHz with the return loss values of -19.26 dB, -25.59 dB, and -23.51 dB, respectively. The L-shaped strips are used to create the third resonant frequency from the antenna design 2. In the fourth geometry, H-shaped-strips were introduced within the rectangular-strips, and resulting shifts of the three resonant frequencies to 2.4 GHz, 3.5 GHz, and 5.5 GHz with their respectively return loss values of -10.39 dB, -28.10 dB, and-13.16 dB.

Finally, by introducing a slot at the ground plane of Figure 1 (d), the proposed multi-band antenna design improves the performance by extending its bandwidth with a minor reduction of the return loss values at three desired frequency bands (2.4 GHz, 3.5 GHz, and 5.5 GHz). The final proposed multi-bands antenna has improved characteristics of return loss, bandwidth, and gain. Figure 2 illustrates the simulated return loss results of antenna 1, antenna 2, antenna 3, and the proposed multi-band antenna.

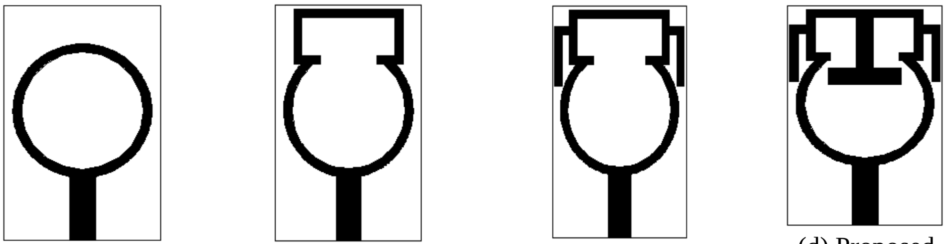

(a) Antenna 1 (b) Antenna 2 (c) Antenna 3 (d) Proposed antenna

**Figure 1:** The geometry of the design process of multi-bands monopole antenna.

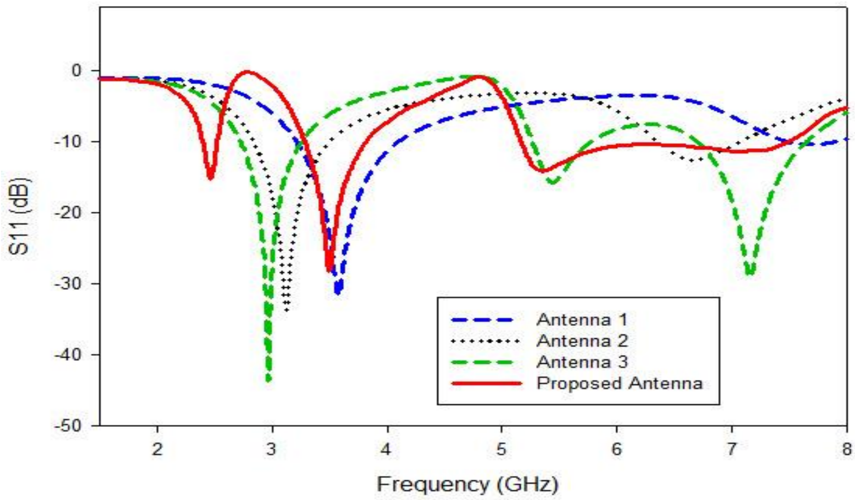


**Figure 2:** Simulated return loss of the proposed antenna.

**Parametric studies**

Based on the afore-mentioned design method, the simulation work was carried out using CST Microwave studio, and results were analyzed. The investigation of the effects of the different structures of the proposed antenna on the impedance matching antenna characteristics, the parametric analysis observed for return loss (S11) results. Therefore, various parameters that affect the antenna characteristics were investigated. In this study, six parameters, namely, $L_1$, $L_{3,}$ $L_4$, $L_{C,}$ $R_{S,}$ and $G_{S,}$ were observed by varying the investigated parameters while keeping other parameters fixed to analyze the S-parameter values.

**Effects of varying distance $L_1$**

The variation of distance $L_1$ affects the design of the proposed multi-band antenna for different lengths. Figure 3 illustrates the return loss results obtained when parameter $L_1$ was varied from 7.2 to 7.7 mm. It can be observed from Figure 3 that, at length, $L_1$ = 7.6 mm, the return loss (S11) values at the resonant frequency of 5.2 GHz is -29.63 dB. The variation of $L_1$ has significant effects on the higher frequency band (5.2/5.5 GHz), while the lower frequency band 2.4/3.5 GHz remains almost unchanged. Thus, strip $L_1$ is mainly used for the creation of a higher resonant frequency. The optimal length of 7.6 mm is used to obtain the desired frequency band, covering 5.2/5.5/5.8 GHz. The simulation results show the impedance bandwidth was 1.04 GHz in the 5.2/5.5/5.8 GHz band for the optimal value of $L_1$.

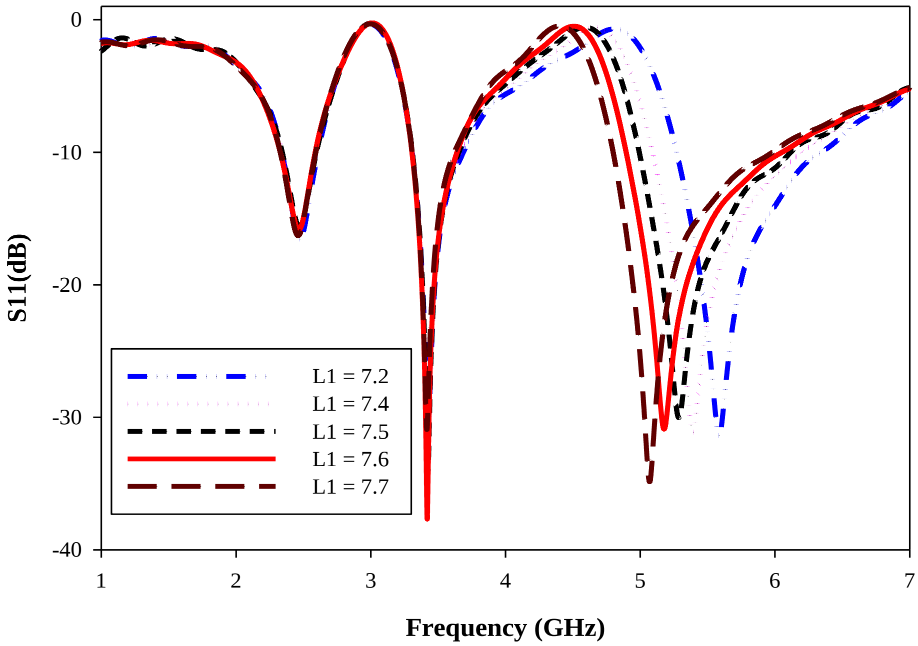


**Figure 3:** Effect of return loss results with the variation of length $L_1$.

**Effects of varying distance $L_3$**

The variation of parameter $L_3$ affects the impedance bandwidth of the antenna. Different simulated return loss results obtained when parameter $L_3$ was varied from 6.5 to 9.5 mm are illustrated in Figure 4. It can be seen that, there is a small increment of the impedance bandwidth at a higher frequency band (5.5

GHz). At the lower value of $L_3$, the resonant frequency at 3.5 GHz and 2.4 GHz shifts to the upper-frequency band, while at a higher length of $L_3$, the resonant frequency shifts to a lower frequency band. Therefore, the variation of parameter $L_3$ shows the effects on the impedance bandwidth of the antenna. The optimum dimension of the parameter $L_3$ was set to 8.5 mm to obtain good impedance bandwidth.

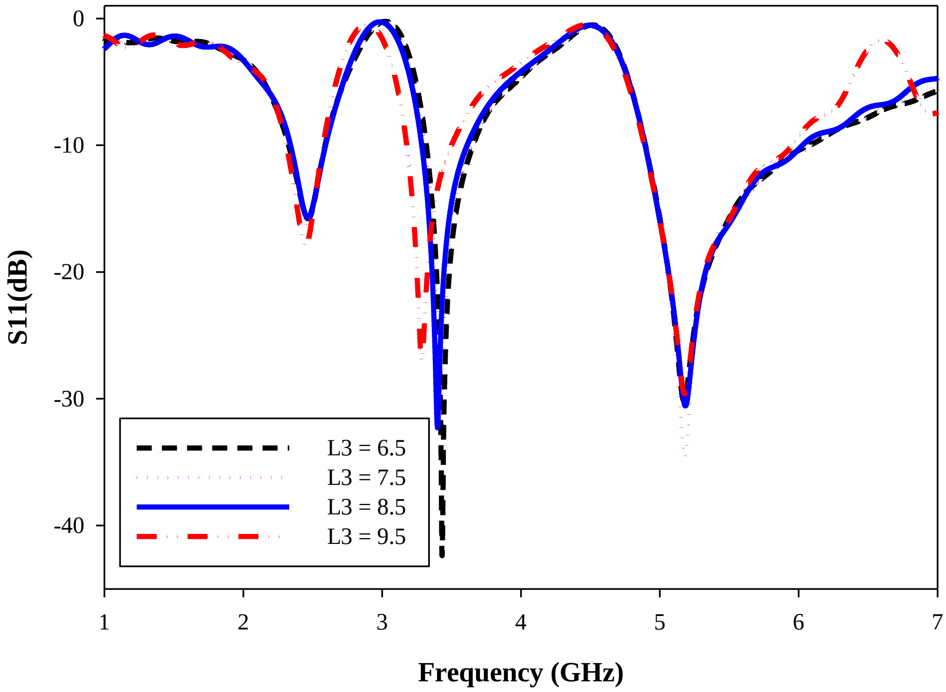


**Figure 4:** Effect of return loss results with the variation of length $L_3$.

**Effects of varying distance $L_4$**

Figure 5 illustrates the simulated return loss results for different lengths of parameter $L_4$. It can be observed that, when $L_4$ varies from 2.6 to 3.2 mm, the impedance bandwidth is not affected at the high-frequency band (5.5 GHz). In comparison, at 2.4 GHz and 3.5 GHz, there are significant effects on its resonant frequencies, where the increase of the length of $L_4$ causes the decrease to its lower values. Therefore, the optimized parameter value of $L_4$ was observed at 3 mm for the desired bandwidth and better antenna performance. It also provides acceptable radiation pattern characteristics.

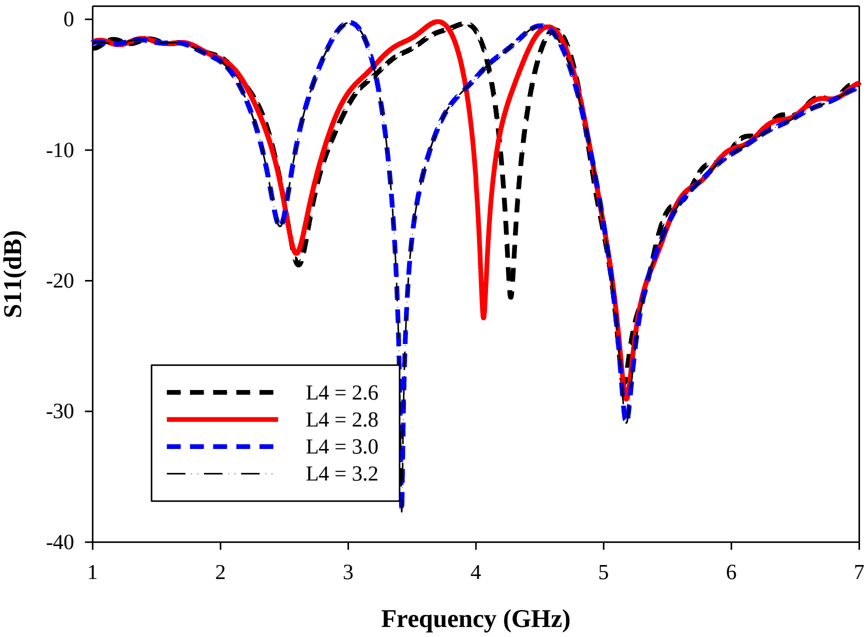


**Figure 5:** Effect of return loss results with the variation of length $L_4$.

**Effects of varying distance $L_C$**

Figure 6 illustrates simulated return loss results on the varying parameter $L_C$. When the value of $L_C$ increases from 8.0 to 11.0 mm, with an interval of 1 mm, there is a decrease of impedance bandwidth at (5.2/5.5 GHz) higher frequency band. At the lower distance of $L_{C,}$ the resonant frequency at 3.5 GHz and 2.4 GHz shifts to the upper-resonant frequency band, while at a higher value of $L_{C,}$ the resonant frequency moves to lower frequency bands. The optimum parameter value for the desired performance was 10.0 mm.

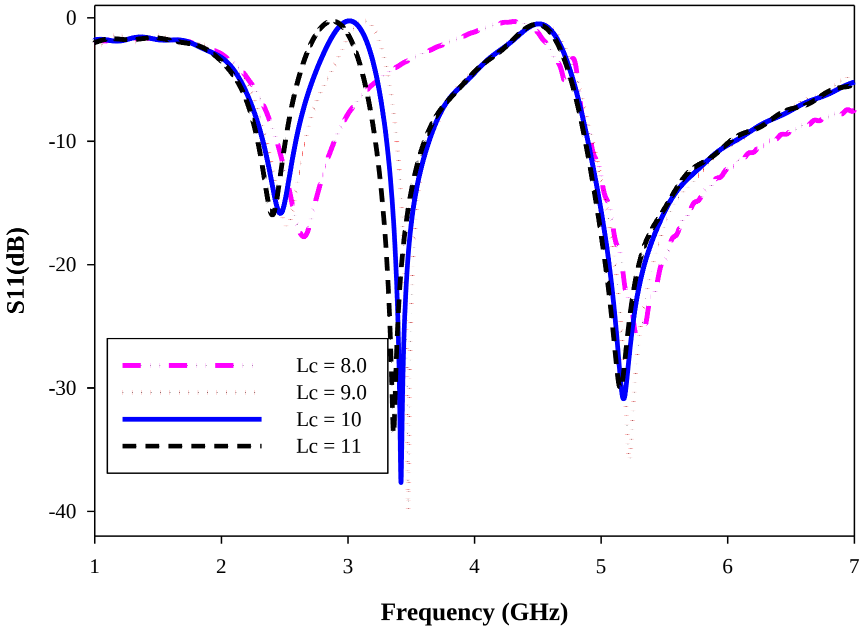


**Figure 6:** Effect of return loss results with the variation of length $L_C$.

**Effects of varying ground slot width $G_S$**

The parameter $G_S$ was varied from 1.5 to 3.5 mm, with an increment of 0.5 mm. Figure 7 shows that the variation of $G_S$ significantly affects the middle frequency band (3.5 GHz) and a higher frequency band (5.5 GHz). In contrast, the lower resonant frequency remains almost constant. The optimum parameter value used was 2 mm.

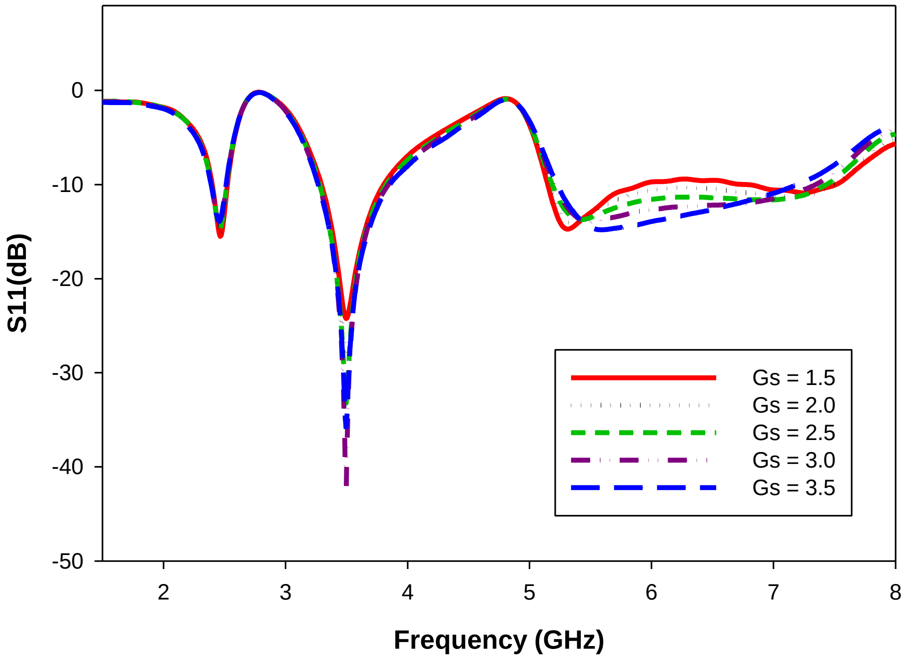


**Figure 7:** Effect of return loss results with the variation of ground slot width $G_s$

**Effects of varying ground slot length $R_S$**

Figure 8 illustrates the simulated return loss results on the variation of parameter $R_S$. From simulated return loss results, it can be observed that changing the value of parameter $R_S$ from 2.5 to 4.5 mm causes significant effects at a higher frequency band by a small increment of return loss value. In contrast, the positions of resonant frequencies at 2.4 GHz and 3.5 GHz remain constant. Therefore, the optimal parameter value used for wide bandwidth was 4 mm.

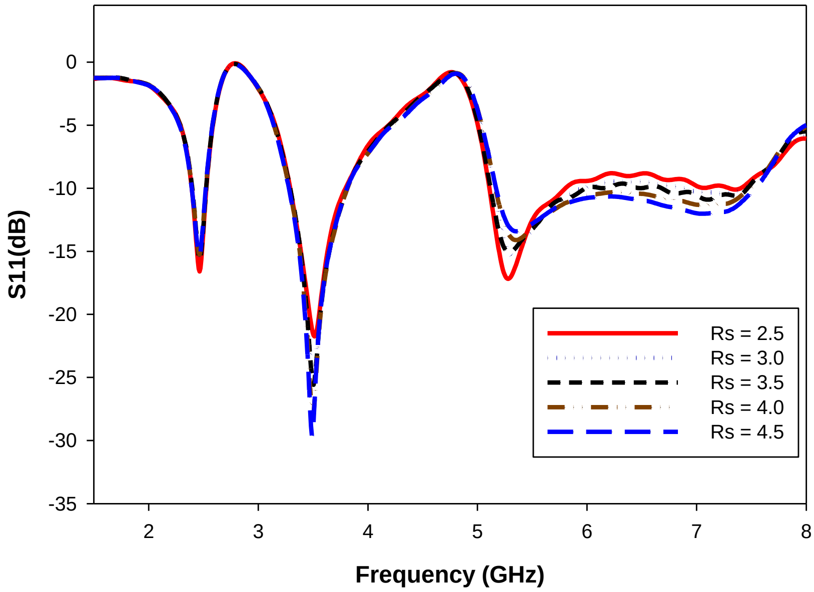


**Figure 8:** Effect of return loss results with the variation of ground slot length $R_s$.

**Proposed multi-band antenna**

Figure 9 (a)-(b) shows the geometry of the proposed multi-band circular ring with a double L-shaped monopole antenna. The antenna has an overall dimension size of 18 mm x 28 mm x 1.6 mm, and its optimized parameters after the parametric analysis are as shown in Table 1.

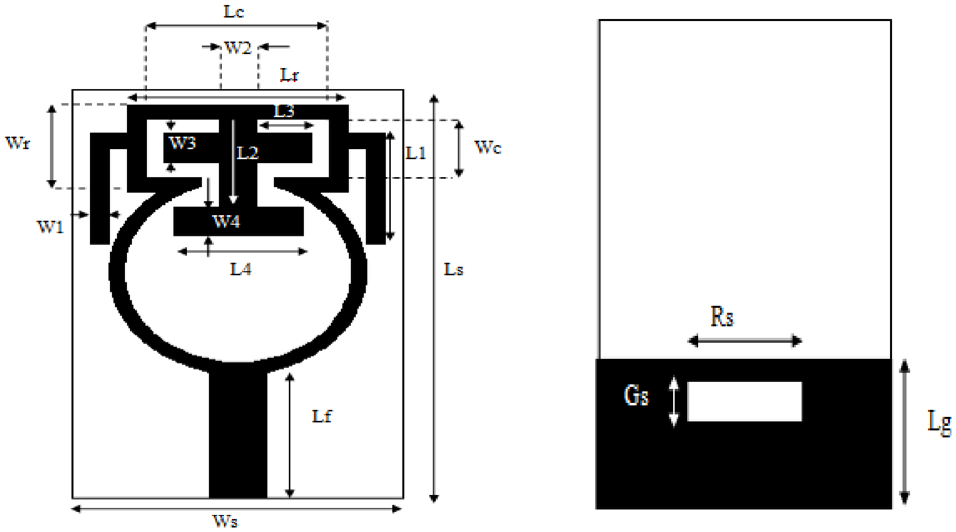


(a) Front view (b) Back view

**Figure 9:** The Geometry of proposed multi-bands antenna.

**Table 1**: The dimension of the proposed antenna

| Parameters | Units (mm) | Parameters | Units (mm) |
|---|---|---|---|
| $L_s$ | 28 | $L_3$ | 3 |
| $W_s$ | 18 | $W_3$ | 2 |
| $L_f$ | 8.7 | $L_4$ | 7 |
| $W_f$ | 3 | $W_4$ | 2 |
| $L_r$ | 12 | $D_1$ | 7 |
| $W_r$ | 6 | $D_2$ | 6.2 |
| $L_1$ | 7.6 | $R_s$ | 7 |
| $W_1$ | 1 | $G_s$ | 2 |
| $L_2$ | 6 | $L_c$ | 10 |
| $W_2$ | 2 | $W_c$ | 4 |

## Results and Discussion

The simulated surface current distributions of the proposed multi-bands monopole antenna are illustrated in Figure 10 (a) – (c) at its resonant frequencies of 2.4 GHz, 3.5 GHz, and 5.5 GHz, respectively. In Figure 10 (a), when the antenna operates at 2.4 GHz, the currents are more distributed on a ring patch element, and in Figure 10 (b), the surface current is distributed along with a ring patch when it operates at 3.5 GHz. Also, Figure 10 (c) shows more current distribution was along with a ring patch, inverted L-shaped strips, and rectangular strip when the antenna operates at 5.5 GHz.

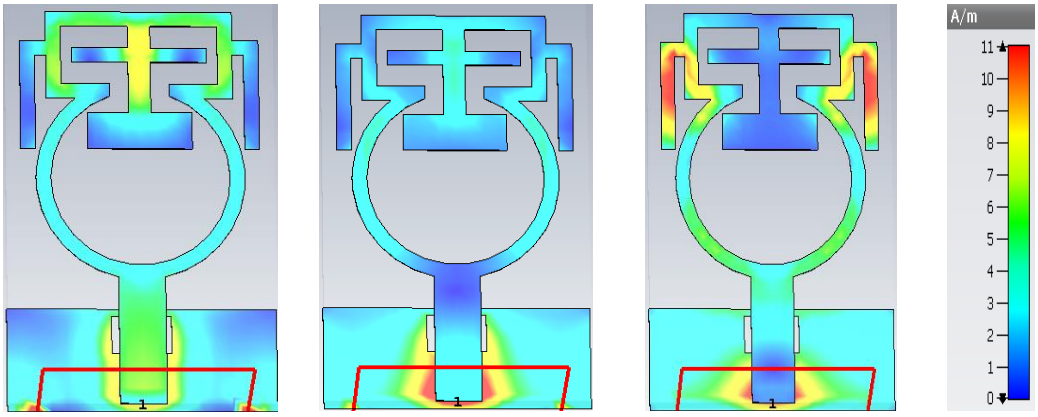


(a) 2.4 GHz (b) 3.5 GHz (c) 5.5 GHz

**Figure 10:** Surface current distribution of the proposed multi-bands antenna at (a) 2.4 GHz, (b) 3.5 GHz, and (c) 5.5 GHz.

Thus, the final optimized dimensions of the proposed circular ring with a double L-shaped antenna were set to 18 x 28 x 1.6 $mm^3$, and its parameters are shown in Table 1. Figure 11 shows the simulated return loss results and -10 dB impedance bandwidth of the proposed circular ring with a double L-shaped multi-band antenna. It can be observed that the simulated results for the antenna provide three resonant frequencies, which were 2.4 GHz, 3.5 GHz, and 5.5 GHz, with return loss values of -10.39 dB, -28.10 dB, and -13.16 dB, respectively. Their corresponding -10 dB impedance bandwidths of 130 MHz (2.39-2.52 GHz), 539 MHz (3.28-3.81 GHz), and 2300 MHz (5.19-7.49 GHz), which cover all WLAN and WiMAX operation bands, were obtained.

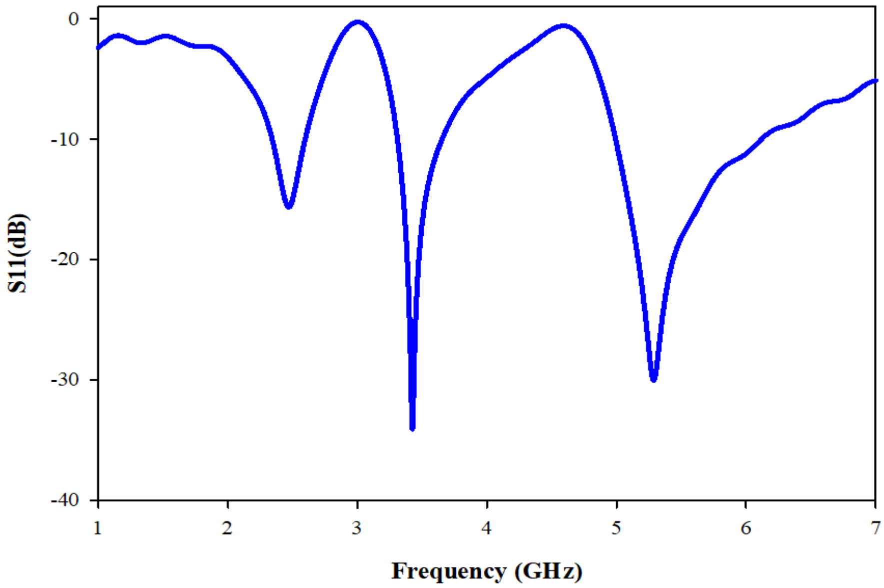


**Figure 11:** Simulated return loss results of the proposed multi-band antenna.

Figures 12, 13, and 14 show the simulated radiation patterns of the proposed antenna for both E-plane and H-plane for 2.4 GHz, 3.5, and 5.5 GHz, respectively. It can be observed from Figures 12, 13, and 14 that the radiation patterns in E-plane has bi-directional patterns and nearly to the omnidirectional radiation pattern in H-plane.

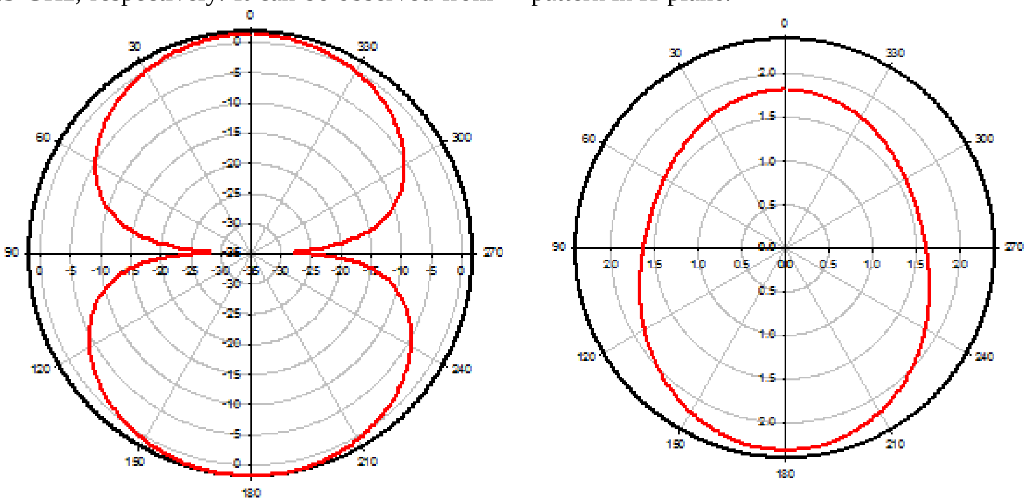


(a) E-Plane (b) H-Plane

**Figure 12:** Simulated radiation patterns at 2.4 GHz.

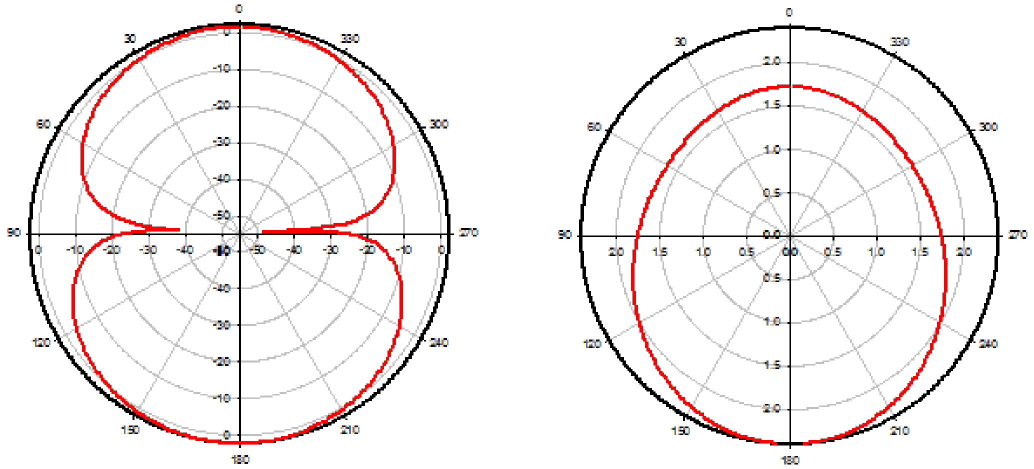

(a) E-Plane (b) H-Plane

**Figure 13:** Simulated radiation patterns at 3.5 GHz.

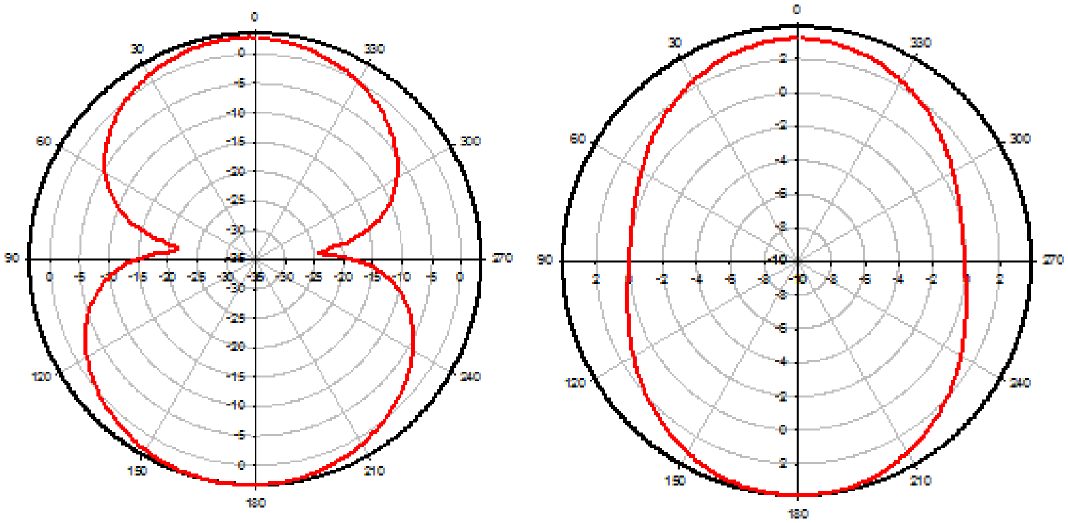

(a) E-Plane (b) H-Plane

**Figure 14:** Simulated radiation patterns at 5.5 GHz.

The simulated antenna gains of the proposed antenna are 1.28 dB, 1.78 dB, and 2.78 dB across three operating frequency bands of 2.4 GHz, 3.5 GHz, and 5.5 GHz, respectively. The simulated far-field radiation patterns of the proposed multi-band antenna are illustrated in Figure 12. The radiations patterns for all of its three frequencies in the E-plane are bi-directional (figure eight), and the radiations patterns in the H-plane are close to omnidirectional.

Table 2 shows the performance comparison of the proposed multi-band antenna with some related works. In contrast with similar antenna designs, the proposed multi-band antenna is small in size and realizes multi-band performance characteristics. The antenna has sufficient impedance bandwidth for covering WLAN (2.4/5.8 GHz) and WiMAX (2.5/3.5/5.5 GHz) operating bands, high antenna gains and good radiation patterns, which can suit a lot of mobile applications.

**Table 2:** Comparative performance of the proposed multi-band antenna with related works reported in the literature

| Related works | Resonant Frequencies (GHz) | Gain (dBi) | Frequency band (GHz) | Size (mm) |
|---|---|---|---|---|
| Song et al. (2011) | 2.4 | 2.3 | 520 MHz (2.32~2.84) | |
| | 3.4 | 2.7 | 960 MHz (3.38~4.34) | 38 × 30 × 1.6 |
| | 5.5 | 4.1 | 800 MHz (5.11~5.91) | |
| Ellis et al. (2014) | 2.5 | 1.0 | 200 MHz (2.50~2.70) | |
| | 3.5 | 1.5 | 320 MHz (3.40~3.72) | 18 × 33 × 1.0 |
| | 5.5 | 1.0 | 1800 MHz (5.00~6.80) | |
| Zhang et al. (2012) | 2.4 | 2.1 | 80 MHz (2.4~2.48) | 30 × 25 × 1.0 |
| | 3.5 | 3.4 | 290 MHz (3.4~3.69) | |
| | 5.5 | 2.1 | 670 MHz (5.15~5.82 ) | |
| Wang et al. (2012) | 2.4 | 2.06 | 150 MHz (2.37~2.52) | 20 × 27 × 1.0 |
| | 3.5 | 2.14 | 330 MHz (3.39~3.72) | |
| | 5.2 | 2.14 | 230 MHz (5.13~5.36) | |
| Chouti et al. (2017) | 2.4 | | 2.33 GHz–2.83 GHz | 36 × 40 × 1.52 |
| | 3.5 | | 3.34 GHz–3.58 GHz | |
| | 5.8 | | 5.5 GHz–5.9 GHz | |
| Huang et al. (2014) | 2.4 | 1.78 | 140 MHz (2.4~2.54) | 20 × 28 × 1.6 |
| | 3.5 | 2.27 | 520 MHz (3.24~3.76) | |
| | 5.5 | 3.63 | 1690 MHz(4.96~6.65) | |
| El Misilmani et al. (2012) | 2.4 | 1.88 | 100 MHz (2.40~2.50) | |
| | 3.5 | 1.85 | 1000 MHz (3.0~4.0) | 25 × 38 × 1.6 |
| | 5.5 | 1.89 | 500 MHz (5.4~5.9) | |
| This study (Proposed multi-band antenna) | 2.4 | 1.28 | 284 MHz (2.327~2.62) | |
| | 3.5 | 1.78 | 368 MHz (3.298~3.62) | 18 × 28 × 1.6 |
| | 5.5 | 2.78 | 1120 MHz(5.19~6.31) | |

**Conclusions**

A multi-band monopole antenna for WLAN/WiMAX applications is presented in this paper. It consists of a circular-shaped strip connected with the rectangular-strip at the top, two inverted L-shaped strips attached outsides of the rectangular-strip. The antenna covers WLAN (2.4/5.2/5.8 GHz) and WiMAX (2.5/3.5/5.5 GHz) frequency bands. The antenna has a small size of only 18 x 28 x 1.6 $mm^3$, including a slot in the ground plane. The results have shown that the antenna achieves the impedance bandwidths of 284 MHz, 368 MHz, and 1120 MHz and the antenna gains of 1.28 dB, 1.78 dB, 2.41 dB, and 2.78 dB for 2.4 GHz, 3.5 GHz, 5.2 GHz, and 5.5 GHz frequency bands, respectively. The simple structure and good radiation patterns of the antenna have various and promising applications for WLAN and WiMAX applications.

**Acknowledgment**

The authors would like to thank the Tanzania Commission for Science and Technology (COSTECH) and the University of Dar es Salaam (UDSM) for financing this study.

**References**

Aghda MR, Kamarudin MR and Iddi HU 2012 M-shape surrounded with ring patch wideband monopole printed antenna. *Microwave Opt. Technol. Lett.* 54(2): 482-486.

Ali T, Khaleeq MM, Pathan S and Biradar RC 2018 A multi-band antenna loaded with metamaterial and slots for GPS/WLAN/WiMAX applications. *Microwave Opt. Technol. Lett.* 60(1): 79-85.

Chetal S, Nayak AK and Panigrahi R 2019 Multiband antenna for WLAN, WiMAX and future wireless applications. *URSI Asia-Pacific Radio Science Conference (AP-RASC)* (pp. 1-4). IEEE, ISBN: 978-1-5386-8551-8.

Chouti L, Messaoudene I, Denidni TA and Benghalia A 2017 Triple-band CPW-fed monopole antenna for WLAN/WiMAX applications. *Progr. Electromagn. Res.* 69: 1-7.

El Misilmani H, Al-Husseini M, Kabalan K and El-Hajj A 2012 A simple miniaturized triple-band antenna for WLAN/WiMAX applications. *Progress in Electromagnetics Research Symposium,* ISBN: 978-1-934142-22-6.

Ellis SM, Zhao, Z, Wu J, Nie ZP and Liu QH 2014 A new compact microstrip-fed monopole antenna for triple band WLAN/WiMAX applications. *Progr. Electromagn. Res.* 48: 129-135.

Fang DG 2009 Antenna theory and microstrip antennas, 1st ed. CRC Press.

Gautam AK, Kumar L, Kanaujia BK and Rambabu K 2015 Design of compact F-shaped slot triple-band antenna for WLAN/WiMAX applications. *IEEE Trans. Antennas Propag.* 64(3): 1101-1105.

Gupta R 2009 Printed tri-band monopole antenna structures for wireless applications. *Microwave Opt. Technol. Lett.* 51(7): 1781-1785.

Huang SS, Li J and Zhao JZ 2014 Compact CPW-fed tri-band antenna for WLAN/WiMAX applications. *Progress in Electromagnetics Res.* 49: 39-45.

Kumar P, Dwari S and Saini RK 2018 Triple band dual polarized CPW-fed planar monopole antenna. *Wireless Pers. Commun.* 99(1): 431-440.

Li F, Ren LS, Zhao G and Jiao YC 2010 Compact triple-band monopole antenna with C-shaped and S-shaped meander strips for WLAN/WiMAX applications. *Progr. Electromagn. Res.* 15: 107-116.

Li WM, Li, WZ, Wu HY, Zhang FS and Zhang SM 2012 A multi-band monopole antenna with two different slots for WLAN and WiMAX applications. *Progr. Electromagn. Res. Lett.* 28: 173-181.

Liu G, Fang M, Zhi R, Bai J and Zeng Z 2017 Compact CPW-fed multi-band antenna for TD-LTE/WLAN/WiMAX applications. *Progr. Electromagn. Res.* 65: 9-14.

Liu WC and Hsu CF 2005 Dual-band CPW-fed Y-shaped monopole antenna for PCS/WLAN application. *Electron. Lett.* 41(7): 390-391.

Mallik KN, Radhika C, Ujwala D, Ramesh H, Kumar AG and Karthik P 2012 A compact microstrip patch antenna with triangular snipped slot for wireless applications. *Int. J. Eng. Adv. Technol. (IJEAT)* 1(4): 116-119.

Pal D, Singhal R, Joshi A and Bandyopadhyay AK 2020 Multiband planar antenna with CSRR loaded ground plane for WLAN and fixed satellite service applications. *Frequenz* 74(11-12): 393-399.

Pandit VK and Harish A 2018 A compact CPW-fed tapered monopole triple-band antenna for WLAN/WiMAX application. *Microwave Opt. Technol. Lett.* 60(9): 2298-2303.

Patel U and Upadhyaya TK 2019 Design and analysis of compact μ-negative material loaded wideband electrically compact antenna for WLAN/WiMAX applications. *Progr. Electromagn. Res.* 79: 11-22.

Pei J, Wang AG, Gao S and Leng W 2011 Miniaturized triple-band antenna with a defected ground plane for WLAN/WiMAX applications. *IEEE Antennas Wireless Propag. Lett.* 10: 298-301.

Raju GN 2009 Antennas and wave propagation, 1st ed, Pearson Education, Canada.

Sang S, Yuan B and Xiang T 2017 Compact tri-band trapezoid CPW-fed antenna with SRR structure for WLAN/WiMAX applications. *Progr. Electromagn. Res.* 61: 177-184.

Saraswat RK and Kumar M 2020 A Quad Band Metamaterial Miniaturized antenna for wireless applications with gain enhancement. *Wireless Pers. Commun.* 114: 3595-3612.

Song ZN, Ding, Y and Huang K 2011 A compact multi-band monopole antenna for WLAN/WiMAX applications. *Progr. Electromagn. Res. Lett.* 23: 147-155.

Thomas KG and Sreenivasan M 2009 Compact triple band antenna for WLAN/ WiMAX applications. *Electron. Lett.* 45(16): 811-813.

Wang T, Yin YZ, Yang J, Zhang YL and Xie JJ 2012 Compact triple-band antenna using defected ground structure for WLAN/WiMAX applications. *Progr. Electromagn. Res.* 35: 155-164.

Weng LH, Guo YC, Shi XW and Chen XQ 2008 An overview on defected ground structure. *Progr. Electromagn. Res.* 7: 173-189.

Yao H, Liu X, Zhu H, Li H, Dong G and Bi K 2020 Dual-band microstrip antenna based on polarization conversion metasurface structure. *Front. Phys.* 8 (279): 1-7

Zhang SM, Zhang FS, Li WM, Li WZ and Wu HY 2012 A multi-band monopole antenna with two different slots for WLAN and WiMAX applications. *Progr. Electromagn. Res.* 28: 173-181.